Electrochemical N_2O Reduction Reaction Catalyzed by a Multinuclear Copper Complex of 1,2,4-Triazole

Zhengwei Ma,[1] Masaru Kato,*[1,2] Takeshi Watanabe[3] and Ichizo Yagi*[1,2]

[1]Graduate School of Environmental Science, Hokkaido University, N10W5, Kita-ku, Sapporo 060-0810, Japan
[2]Faculty of Environmental Earth Science, Hokkaido University, N10W5, Kita-ku, Sapporo 060-0810, Japan
[3] Industrial Application and Partnership Division, Japan Synchrotron Radiation Research Institute (JASRI), SPring-8, 1-1-1 Kouto, Sayo 679-5198, Japan.
*Corresponding authors: Graduate School of Environmental Science, Hokkaido University, N10W5, Kita-ku, Sapporo 060-0810, Japan; Faculty of Environmental Earth Science, Hokkaido University, N10W5, Kita-ku, Sapporo 060-0810, Japan. Email: *masaru.kato@ees.hokudai.ac.jp* (M.K.), *iyagi@ees.hokudai.ac.jp* (I.Y.).

Abstract

A trinuclear copper complex of 1,2,4-triazole supported on a carbon black efficiently catalyzes the electrochemical N_2O reduction reaction (e-N_2ORR) in alkaline media, achieving 100% Faradaic efficiency at -0.2 V vs. RHE and a turnover frequency up to 267 h^{-1} at -0.6 V vs. RHE. *In situ* X-ray absorption spectroscopy reveals that a Cu(0) species produced from the Cu(II) complex under electrochemical conditions is responsible for the high e-N_2ORR activity and selectivity, offering a cost-effective strategy for efficient greenhouse gas mitigation.

Keywords: N_2O reduction, electrocatalysis, denitrification

Graphical abstract

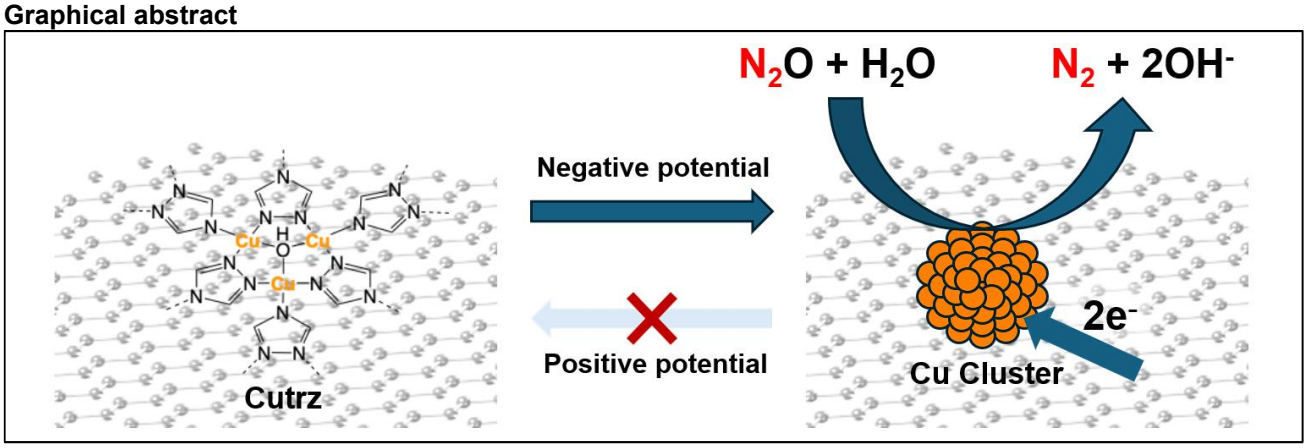

Nitrous oxide (N_2O) is a frequently overlooked greenhouse gas, despite possessing a global warming potential approximately 273 times greater than that of CO_2 with long lifetime over 110 years.[1–4] Anthropogenic sources of N_2O have exceeded the natural atmospheric sink capacity, resulting in a continuous increase in atmospheric N_2O concentrations at a rate of approximately 1 ppb per year.[5] Of greater concern is that this upward trend is accelerating.[1,5] Therefore, efficient and cost-effective methods for N_2O removal should be developed.

N_2O can be removed in various ways. Thermal decomposition in the absence of a catalyst is highly energy-intensive, typically requiring temperatures above 600 °C.[6,7] Thermal decomposition not only requires high energy input but also involves the use of reducing agents, which may cause secondary pollution and add to the overall cost.[8] Despite eliminating secondary pollution and reducing the operating temperature compared to thermal decomposition, direct catalytic decomposition still requires temperatures exceeding 300 °C.[1,9]

Electrochemical N_2O reduction reaction (e-N_2ORR) converts N_2O into harmless N_2 powered by renewable energy sources in ambient condition without secondary pollution. Palladium-based catalysts have been widely employed for the e-N_2ORR to N_2 indicating almost 100% Faradaic efficiency (FE) with higher onsetpotential than other metal and potential for further improvement.[10,11] Alloying Pd with other metals has also been explored as an effective strategy to promote reactant adsorption but suppressing competing hydrogen adsorption, thereby enhancing the e-N_2ORR activity.[12–15] However, the scarcity and high cost of

palladium remain significant barriers to its large-scale application in e-N_2ORR.

Non-noble metal-based electrocatalysts for the e-N_2ORR have been intensively developed including single-atom and molecular-based electrocatalysts.[13–15] A copper-based single-atom catalyst (SAC) of atomically dispersed Cu, N-doped carbon (Cu-N-C) exhibited a high N_2 yield rate of 3.53 mmol h^{-1} mg_{metal}^{-1}, corresponding to a turnover frequency (TOF) of 224 h^{-1} at –0.5 V vs. the reversible hydrogen electrode (RHE) and the optimal 82.1% FE at –0.2 V vs. RHE to N_2.[16] As molecular-based electrocatalysts, a copper complex with 2,6-(bis(bis-2-*N*-methylimidazolyl)phosphino) pyridine) exhibits a TOF of 53 h^{-1} with >83% FE.[17] Recently, a dinuclear copper complex with 3,5-diamino-1,2,4-triazole, which was inspired by the active site of nitrous oxide reductases, was reported to show a TOF of 110 h^{-1} and almost 100% FE at –0.3 V vs. RHE.[18] An iron complex with tetraphenylporphyrin shows a TOF of 3.93 h^{-1} with 100% FE.[19] These findings demonstrate the great potential of non-noble metal-based electrocatalysts for the efficient and selective e-N_2ORR.

In this work, we employed a multinuclear copper complex of 1,2,4-triazole (Cutrz) supported by a carbon black of Ketjenblack EC-600JD (KB),[20] named Cutrz/KB, for the e-N_2ORR. Cutrz/KB exhibited an outstanding selectivity and TOF. The potential-dependent X-ray absorption spectroscopy (XAS) of Cutrz/KB has been conducted to identify the active species for the e-N_2ORR

Cutrz/KB was prepared following a previously reported procedure, as illustrated in **Fig 1**.[20] Cutrz/KB was obtained by mixing $CuCl_2{\cdot}2H_2O$,1,2,4-triazole and KB in water under stirring at room temperature overnight, vacuum filtration, and vacuum drying at room temperature. Powdery X-ray diffraction analysis of Cutrz/KB (**Fig. S1**) confirms the successful loading of Cutrz onto KB. Characteristic diffraction lines of crystalline Cutrz[20] are retained in the Cutrz/KB composite, while a broad hump at 2θ around 25° and 45° indicates the presence of amorphous carbon from KB.[21]

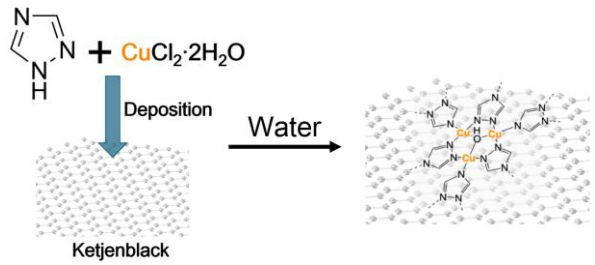

Fig.1. Schematic representation of the preparation procedure of Cutrz/KB.

Cyclic voltammograms (CVs) of Cutrz/KB were recorded in Britton-Robinson (BR) buffered aqueous solutions containing 0.1 M $NaClO_4$ under N_2O and Ar at different pHs to find out the optimal condition for the e-N_2ORR (**Fig S2**). Cathodic currents were observed at onset potentials of about −0.5 V vs. RHE in the CVs under Ar, indicating the hydrogen evolution reaction (HER). In the CVs under N_2O, cathodic currents with more positive onset potential were observed, indicating that the Cutrz/KB shows the e-N_2ORR activity. The current density difference between the HER and e-N_2ORR was maximized at pH 13 (**Fig. S2**). Thus, Cutrz/KB shows the highest e-N_2ORR activity at pH 13. The subsequent experiments were carried out at pH 13.

The selective production of N_2 catalyzed by Cutrz/KB for the e-N_2ORR at ≤−0.2 V vs. RHE was confirmed by chronoamperometry (**Fig. S3a**) coupled with online gas chromatography. TOFs and FE of Cutrz/KB for the e-N_2ORR at different potentials are summarized in **Figs. 2a** and **2b**, respectively. N_2 was the sole product at –0.2 V vs. RHE (**Fig. S4c**), and the FE reaches 100%. At more negative potentials, the HER begins to compete, leading to a gradual decrease in N_2 selectivity: the FE for N_2 decreases from ~87% at –0.3 V, to ~70% at –0.4 V, to ~40% at –0.5 V, and finally to ~38% at –0.6 V vs. RHE. This indicates that both HER and e-N_2ORR proceed at ≤−0.3 V vs. RHE. A similar trend has been observed for Cu foil, Cu nanoparticles (Cu NPs), and Cu–N–C, where the FE for the N_2 formation decreases at more negative potentials due to the competing HER.[16]

The TOFs were calculated based on the electrochemically active copper sites determined from the integrated charge (0.65 C) associated with the $Cu^{II/I}$ redox couple in the CV under Ar (**Fig. S3b**), corresponding to 0.54 μmol cm^{-2} and 90% of the total loading amounts of Cu ions of Cutrz/KB. The TOFs to N_2 increase as more negative potentials are applied: 73 h^{-1} at -0.2 V; 165 h^{-1} at -0.3 V; 210 h^{-1} at –0.4 V; to 237 h^{-1} at -0.5 V; and finally to a maximum of 267 h^{-1} at -0.6 V vs. RHE (**Fig. 2b**).

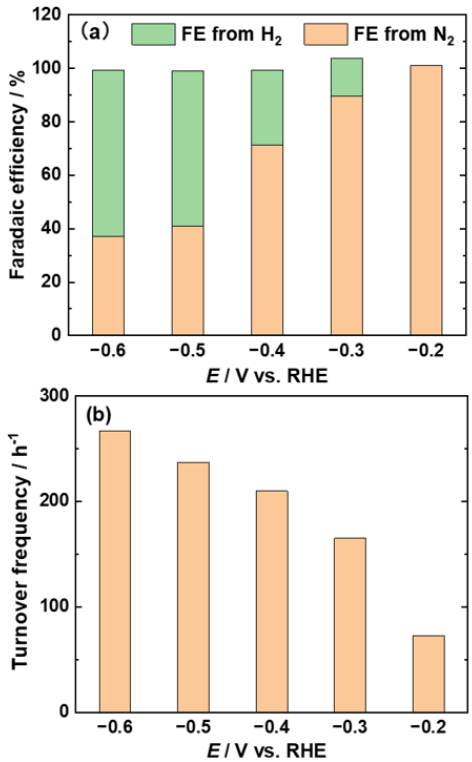

Fig. 2. Potential dependence of (a) FEs to H_2 (in green) and N_2 (in orange) and (b) TOFs of Cutrz/KB to N_2 in the BR buffered aqueous solution at pH 13 under N_2O.

Cutrz/KB outperforms previously reported Cu-based electrocatalysts in terms of both FEs and TOFs.[16,17] Between –0.2 and –0.5 V vs. RHE, Cutrz/KB demonstrates higher FEs (100-40%) and TOFs (73-237 h^{-1}) than Cu NPs (65-20%FE and TOFs of 88.9-139 h^{-1}).[16] Cutrz/KB also achieves notably higher FEs maintaining comparable or slightly superior TOFs ranging from -0.2 to -0.5 V vs. RHE than Cu-N-C (82-46%FE and TOFs of 114-224 h^{-1}).[16] Furthermore, the FE and TOF of the mononuclear Cu complex of 2,6-(bis(bis-2-*N*-methylimidazolyl)phosphino)pyridine are significantly lower than those of Cutrz/KB (FE = 87% and TOF = 165 h^{-1} at –0.3 V).[17] Although Cutrz/KB exhibited lower FE than the dinuclear copper complex with 3,5-diamino-1,2,4-triazole within the potential range of -0.3 to -0.6 V vs. RHE, and also displayed a lower TOF at potentials at -0.4, -0.5, and -0.6 V vs. RHE, its TOF at -0.3 V vs. RHE (165 h^{-1}) exceeded that of the dinuclear copper complex (110 h^{-1}) at the same potential.[18] These results indicate that Cutrz/KB offers a more favorable balance between catalytic activity and selectivity toward N_2 formation for the e-N_2ORR.[16-17]

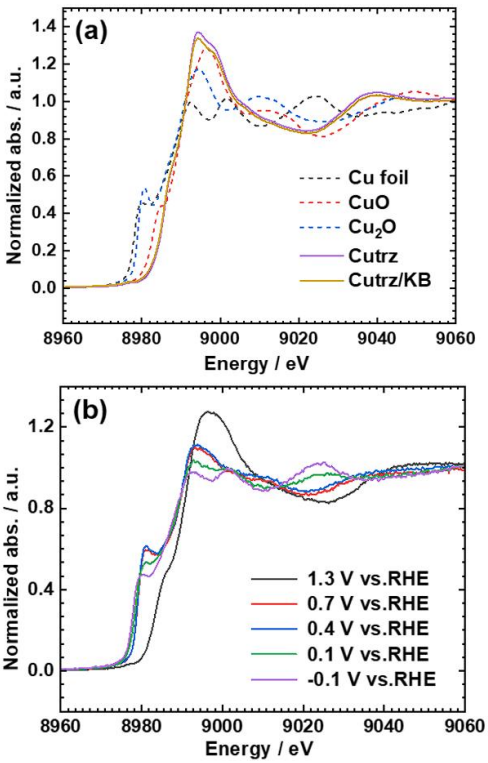

Fig. 3. (a) Cu *K*-edge XANES spectra of Cutrz (the solid line in purple), Cutrz/KB (the solid line in brown) and reference samples of Cu foil (the broken line in black), Cu_2O (the broken line in blue), and CuO (the broken line in red); (b) *In situ* Cu *K*-edge XANES spectra of Cutrz/KB at various applied potentials at pH 13.

Ex situ XAS data of Cutrz/KB in the Cu *K*-edge X-ray absorption near edge structure (XANES) region were recorded to investigate the initial oxidation state of copper ions in Cutrz/KB. The comparison of the XANES spectrum of Cutrz/KB with those of the reference samples shows that the absorption edge position of Cutrz resembles that of CuO (Fig. 3a), indicating the initial oxidation state of copper ions in Cutrz/KB is Cu(II). The nearly identical spectra of Cutrz and Cutrz/KB suggest that KB has no influence on the initial oxidation state of Cu. This result is in good agreement with previously reported results.[22]

The potential-dependent XANES spectra of Cutrz/KB revealed oxidation state changes of copper ions under electrochemical conditions (Fig. 3b and Fig. S5). As the applied potential negatively changed from +1.3 to +0.4 V vs. RHE, the characteristic peak located at 8981 eV appeared. This peak is assigned to the 1s → $4p_\pi$ transition of Cu(I) ions, suggesting that Cu(II) ions were electrochemically reduced to Cu(I) ions in Cutrz/KB.[23] At more negative potentials, characteristic features appeared at 8979, 9002, and 9024 eV, indicating the further reduction to metallic Cu(0).[24] This transformation was further corroborated by the comparison of extended X-ray absorption fine structure (EXAFS) oscillations (Fig. S6a) and Fourie transforms of

EXAFS (FT-EXAFS) oscillations (**Fig. S6b**) between Cutrz/KB at -0.1 V vs. RHE and Cu foil. The phases of these of the EXAFS oscillation between Cutrz/KB (-0.1 V vs. RHE and pH 13) and the Cu foil are the same (**Fig. S6a**), indicating that the local coordination environment of Cutrz/KB under the reductive condition closely resembles that of metallic copper. FT-EXAFS oscillations (**Fig. S6b**) also revealed the change in the first coordination sphere from Cu–N to Cu–Cu coordination at -0.1 V vs. RHE for Cutrz/KB. Curve fitting analysis of FT-EXAFS oscillations (**Table S1**) gave the Cu–Cu path with 2.53±0.01 Å and a coordination number (CN) of 9.52±0.04, which is lower than that of Cu foil (CN=12). This result indicates the formation of Cu clusters with the number of Cu atoms close to 309, where 162 surface Cu atoms with an average CN of 7.2 are exposed.[25,26] Abundant low-coordinated Cu sites are recognized in catalysis as a key structural feature for enhanced activity.[27–29] Constructing low-coordinated Cu sites has been proven as an effective strategy to tailor the adsorption energy of inter mediate catalytic species towards more effective electrocatalytic rates.[30] For example, in CO and CO_2 electroreduction, tuning the CN to modulate the strength of chemisorption has been shown to enhance catalytic activity.[25,29] The Cu(0) cluster possibly acts as the active species for the e-N_2ORR.

Such a Cu(0) cluster does not form at pH 7. *In situ* XAS spectra at pH 7 (**Fig. S5**) showed shifts of the absorption edge to lower energies, indicating the reduction of Cu(II) to Cu(I). Even at -0.35 V vs. RHE, which is more negative than the potentials showing the Cu(0) cluster formation of Cutrz/KB at pH 13, no evidence for the formation of metallic Cu(0) was found. These results indicate that the Cutrz framework remains intact with the Cu(I) centers. These observations suggest that alkaline conditions facilitate the formation of the Cu(0) cluster, which may account for the enhanced e-N_2ORR activity observed under alkaline conditions.

In conclusions, we employed the trinuclear Cu complex of Cutrz supported on KB as an efficient and non-noble electrocatalyst for the e-N_2ORR in alkaline media. Cutrz/KB achieves the 100%FE and the TOF of 73 h^{-1} at -0.2 V vs. RHE and the maximum TOF of 267 h^{-1} at -0.6 V vs. RHE at pH 13. Potential-dependent XAS data revealed that the high activity originates from Cu(0) produced from the stepwise reduction of the Cu(II) ions of Cutrz via the Cu(I) ions. The resulting Cu(0) clusters serve as highly active and selective reaction centers for the e-N_2ORR to N_2. This study highlights a promising strategy for the design of cost-effective and efficient electrocatalysts based on based on non-precious metals for N_2O mitigation at ambient conditions.

Supplementary data

Supplementary material is available at *Chemistry Letters*

Funding

This work was supported by EXEX doctoral fellowship, JFE 21st Century Foundation, JSPS KAKENHI (Grant numbers 19H02664 and 21K05124), "Advanced Research Infrastructure for Materials and Nanotechnology (ARIM)" programs of MEXT for Hokkaido University (JPMXP1222HK0033, JPMXP1223HK0012, JPMXP1224HK0036 and JPMXP1225HK0022). Synchrotron radiation experiments were performed at the BL14B2 of SPring-8 with the approval of the Japan Synchrotron Radiation Research Institute (JASRI) (Proposal nos. 2023A1791 and 2023B1916).

Conflict of interest statement. None declared

References

1 M. Konsolakis, *ACS Catal.* **2015**, *5*, 6397–6421.
2 S.R. Pauleta, M.S.P. Carepo and I. Moura, *Coord. Chem. Rev.* **2019**, *387*, 436–449.
3 M. Strokal and C. Kroeze, *Curr. Opin. Environ. Sustain.* **2014**, *9–10*, 108–121.
4 L. Li, J. Xu, J. Hu and J. Han, *Environ. Sci. Technol.* **2014**, *48*, 5290–5297.
5 Global Monitoring Laboratory, "Trends in Atmospheric Nitrous Oxide (N_2O)", can be found under https://gml.noaa.gov/ccgg/trends_n2o, **2024**.
6 X. Wang, R. Duan, Z. Li, M. Gao, Y. Fu, Y. Han, G. He and H. He, *Environ. Sci. Technol.* **2025**, *59*, 5839–5847.
7 A. Shimizu, K. Tanaka and M. Fujimori, *Chemosphere – Global Change Sci.* **2000**, *2*, 425–434.
8 M. Inger, B. Moszowski, M. Ruszak, J. Rajewski and M. Wilk, *Catalysts* **2020**, *10*, 987.
9 Z. Zhuang, B. Guan, J. Chen, C. Zheng, J. Zhou, T. Su, Y. Chen, C. Zhu, X. Hu, S. Zhao, J. Guo, H. Dang, Y. Zhang, Y. Yuan, C. Yi, C. Xu, B. Xu, W. Zeng, Y. Li, K. Shi and Z. Huang, *Chem. Eng. J.* **2024**, *486*, 150374.
10 A. Kudo and A. Mine, *J. Electroanal. Chem.* **1996**, *408*, 267–269.
11 B.H. Ko, B. Hasa, H. Shin, Y. Zhao and F. Jiao, *J. Am. Chem. Soc.* **2022**, *144*, 1258–1266.
12 A.C. Sarker, M. Kato, M. Kawamura, T. Watanabe and I. Yagi, *Catal. Sci. Technol.* **2024**, *14*, 4137–4141.
13 A.C. Sarker, M. Kato and I. Yagi, *Electrochim. Acta* **2022**, *425*, 140628.
14 S. Baek, K. Kim, O.S. Kwon, H. Kim, J.W. Han, O.J. Kwon and J.J. Kim, J. Appl. Electrochem. **2020**, *50*, 395–405.
15 M. Kato, J. Zheng, Y. Deng, F. Saito, Y. Unuma, S. Oka, K. Tamura and I. Yagi, *ACS Catal.* **2025**, *15*, 7710–7719.
16 Z. Li, Y. Wu, H. Wang, Z. Wu and X. Wu, *Environ. Sci. Technol.* **2024**, *58*, 8976–8987.
17 J.L. Martinez, J.E. Schneider, S.W. Anferov and J.S. Anderson, *ACS Catal.* **2023**, *13*, 12673–12680.
18 Z. Ma, M. Kato, J. Pirillo, Y. Hijikata, T. Watanabe, Y. Uemura, B. Lu, S. Takakusagi, K. Kimijima, *Angew. Chem. Int. Ed.* **2025**, e202506067.
19 J.S. Stanley, X.S. Wang and J.Y. Yang, *ACS Catal.* **2023**, *13*, 12617–12622.
20 T. Yamada, G. Maruta and S. Takeda, *Chem. Commun.* **2011**, *47*, 653–655.
21 U. A. do Rêgo, R. Sgarbi, T. Lopes, C. C. dos Santos, A. A. Tanaka, E. A. Ticianelli, *Electrocatalysis* **2021**, *12*, 548-563.

22 M. Kato, M. Muto, N. Matsubara, Y. Uemura, Y. Wakisaka, T. Yoneuchi, D. Matsumura, T. Ishihara, T. Tokushima, S. Noro, S. Takakusagi, K. Asakura and I. Yagi, *ACS Appl. Energy Mater.* **2023**, *13*, 9736–9747.

23 M. Kato, K. Kimijima, M. Shibata, H. Notsu, K. Ogino, K. Inokuma, N. Ohta, H. Uehara, Y. Uemura, N. Oyaizu, T. Ohba, S. Takakusagi, K. Asakura and I. Yagi, *Phys. Chem. Chem. Phys.* **2015**, *17*, 8638–8641.

24 Q. Chang, J.H. Lee, Y. Liu, Z. Xie, S. Hwang, N.S. Marinkovic, A.H.A. Park, S. Kattel and J.G. Chen, *JACS Au* **2022**, *2*, 214–222.

25 F.A. Rollier, V. Muravev, A. Parastaev, R.C.J. van de Poll, J.M.J.J. Heinrichs, B. Ligt, J.F.M. Simons, M.C. Figueiredo and E.J.M. Hensen, *ACS Catal.* **2024**, *14*, 13246–13259.

26 R.E. Benfield, *J. Chem. Soc., Faraday Trans.* **1992**, *88*, 1107–111.

27 Y. Yang, S. Louisia, S. Yu, J. Jin, I. Roh, C. Chen, M.V. Fonseca Guzman, J. Feijóo, P.C. Chen, H. Wang, C.J. Pollock, X. Huang, Y.T. Shao, C. Wang, D.A. Muller, H.D. Abruña and P. Yang, *Nature* **2023**, *614*, 262–269.

28 X. Feng, K. Jiang, S. Fan and M.W. Kanan, *ACS Cent. Sci.* **2016**, *2*, 169–174.

29 R. Reske, H. Mistry, F. Behafarid, B. Roldan Cuenya and P. Strasser, *J. Am. Chem. Soc.* **2014**, *136*, 6978–6986.

30 X. Li, S. Wang, L. Li, Y. Sun and Y. Xie, *J. Am. Chem. Soc.* **2020**, *142*, 9567–9581